Modeling the impact of quarantine during an outbreak of Ebola virus disease

Attila Dénes [a, *], Abba B. Gumel [b, 1]

[a] Bolyai Institute, University of Szeged, Aradi vértanúk tere 1., Szeged H-6720, Hungary
[b] School of Mathematical and Statistical Sciences, Arizona State University, Tempe, AZ 85287-1804, USA

A B S T R A C T

The quarantine of people suspected of being exposed to an infectious agent is one of the most basic public health measure that has historically been used to combat the spread of communicable diseases in human communities. This study presents a new deterministic model for assessing the population-level impact of the quarantine of individuals suspected of being exposed to disease on the spread of the 2014—2015 outbreaks of Ebola viral disease. It is assumed that quarantine is imperfect (i.e., individuals can acquire infection during quarantine). In the absence of quarantine, the model is shown to exhibit global dynamics with respect to the disease-free and its unique endemic equilibrium when a certain epidemiological threshold (denoted by $\mathscr{R}_0$) is either less than or greater than unity. Thus, unlike the full model with imperfect quarantine (which is known to exhibit the phenomenon of backward bifurcation), the version of the model with no quarantine does not undergo a backward bifurcation. Using data relevant to the 2014—2015 Ebola transmission dynamics in the three West African countries (Guinea, Liberia and Sierra Leone), uncertainty analysis of the model show that, although the current level and effectiveness of quarantine can lead to significant reduction in disease burden, they fail to bring the associated *quarantine reproduction number* ($\mathscr{R}_0^Q$) to a value less than unity (which is needed to make effective disease control or elimination feasible). This reduction of $\mathscr{R}_0^Q$ is, however, very possible with a modest increase in quarantine rate and effectiveness. It is further shown, *via* sensitivity analysis, that the parameters related to the effectiveness of quarantine (namely the parameter associated with the reduction in infectiousness of infected quarantined individuals and the contact rate during quarantine) are the main drivers of the disease transmission dynamics. Overall, this study shows that the singular implementation of a quarantine intervention strategy can lead to the effective control or elimination of Ebola viral disease in a community if its coverage and effectiveness levels are high enough.

* Corresponding author.
  E-mail address: denesa@math.u-szeged.hu (A. Dénes).
  Peer review under responsibility of KeAi Communications Co., Ltd.
[1] Other affliation: Department of Mathematics and Applied Mathematics, University of Pretoria, Pretoria 0002, South Africa

1. Introduction

Ebola virus disease (EVD), which first appeared in 1976 in Zaire (Bowen et al., 1977; Johnson, Webb, Lange, & Murphy, 1977), is one of the most virulent viral diseases of humans, with a case fatality ratio estimated between 25 and 90% (World Health Organization, 2018a). EVD is transmitted between humans through contact with blood, secretions, organs or other bodily fluids of infected or dead humans or animals, and its incubation period range between 2 and 21 days. The symptoms are vomiting, diarrhea, body rash, tremors and in some cases, both internal and external bleeding. The largest Ebola outbreak so far started in Guinea in December 2013 (World Health Organization, 2015). During this epidemic, almost 29,000 people contracted the disease which resulted in more than 11,000 deaths, mostly in Guinea, Liberia and Sierra Leone. A new outbreak started recently (on 4 April 2018) in the Democratic Republic of the Congo and (as of October 20, 2018) there have already been 237 Ebola cases and 153 deaths (World Health Organization, 2018b).

Quarantine, defined loosely as the temporary removal (from their immediate abode or the general population) of people suspected of being exposed to a communicable disease, has historically been used as an effective basic public health control measure to prevent the spread of infectious diseases. There are numerous issues pertaining to the logistic of the actual implementation of quarantine as a control strategy, such as who should be quarantined and for how long suspected people should be in quarantine (these have major socio-economic and public health implications). For instance, in the case of the 2014 outbreaks of the EVD, some US states imposed a three-week quarantine period for all health care workers who returned to the United States from the Ebola-affected regions (where they may have cared for patients with Ebola) (Campbell, Adan, & Morgado, 2017; Drazen et al., 2014). It was, however, shown by Haas (Haas, 2014) that the three-week period may not be optimal (in particular, it was shown that exposed individuals with 0.2%–12% risk of developing disease may be released from quarantine prior to the end of the incubation period). On August 1, 2014, the three Western African countries affected by the epidemic (Guinea, Liberia and Sierra Leone) announced the enforcement of a mass quarantine in vast forest areas around their common borders that are considered the epicentre of the outbreak (a few days later, Liberian authorities imposed a 10-day quarantine over West Point; Sierra Leone announced, on September 6, a nationwide mass quarantine between September 19 and 21) (Eba, 2014).

Numerous mathematical modeling studies have been conducted to study the transmission dynamics and control of EVD. In fact, the earliest mathematical models for EVD appeared long before the 2014–15 epidemic. Chowell et al. (Chowell, Hengartner, Castillo-Chavez, Fenimore, & Hyman, 2004) proposed a stochastic SEIR model to fit data from the 1995 and 2000 outbreaks in Congo and Uganda. This model was further developed by Legrand et al. (Legrand, Grais, Boelle, Valleron, & Flahault, 2007) by including two new compartments for hospitalized people and for people who died from Ebola but have not yet been buried. Several new models appeared soon after the start of the 2014 outbreak (Nishiura & Chowell, 2014; Towers, Patterson-Lomba, & Castillo-Chavez, 2014). The model by Legrand et al. was used to study the 2014–15 Ebola outbreaks by Rivers et al. (Rivers, Lofgren, Marathe, Eubank, & Lewis, 2014). Webb and Browne incorporated age of infection in their model (Webb & Browne, 2016). Tsanou et al. considered the role of host-reservoir transmission (with bats as reservoir) of EVD and spillover potential to humans (Tsanou, Bowong, Lubuma, & Mbang, 2017). Furthermore, Tsanou et al. (Tsanou, Lubuma, Ouemba Tassé, & Tenkam, 2018) studied the impact of environmental contamination on the transmission dynamics of EVD. Several other studies incorporated the effect of anti-EVD control measures, such as increasing hospitalization, timely burial of people who died from EVD and distribution and use of protective kits in households (Althaus, 2014; Barbarossa et al., 2015; Lewnard et al., 2014). For instance, Agusto et al. (Agusto, Teboh-Ewungkem, & Gumel, 2015) studied the effect of traditional beliefs and customs on the transmission dynamics of the disease.

A number of mathematical models, typically of the form of deterministic systems of nonlinear differential equations, have been designed and used to gain insight into the population-level impact of quarantine (of people suspected of being exposed to a disease) and isolation (of people with clinical symptoms of a communicable disease) on the spread and control of infectious diseases (see, for instance, the models in (Day, Park, Madras, Gumel, & Wu, 2006; Gumel et al., 2004; Hethcote, Zhien, & Shengbing, 2002; Lipsitch et al., 2003; Mubayi, Kribs Zaleta, Martcheva, & Castillo-Chávez, 2010; Nuño, Feng, Martcheva, & Castillo-Chavez, 2005; Safi & Gumel, 2010; Safi & Gumel, 2013; Safi & Gumel, 2015; Yan & Zou, 2008)). Hethcote (Hethcote et al., 2002) presented SIQS (susceptible-infected-quarantined-susceptible) and SIQR (susceptible-infected-quarantined-recovered) models for the dynamics of an infectious disease that is controllable using quarantine and isolation, showing that the use of quarantine-adjusted incidence induces the phenomenon of Hopf bifurcation in the transmission dynamics of the disease. Nuño et al. (2005) also showed oscillatory dynamics in an SIQR model for the dynamics of two strains of influenza in a population. Similarly, a probabilistic model was designed and used by Day et al. (Day et al., 2006) to determine the conditions under which quarantine is expected to be useful. The Day et al. study showed that the number of infections averted through quarantine is expected to be low if isolation is effective, but the number increases abruptly as the effectiveness of isolation diminishes. It is worth mentioning, however, that in majority of the quarantine, or quarantine and isolation, models in the literature (including the models in all of the aforementioned studies, with exception of those in (Lipsitch et al., 2003; Mubayi et al., 2010; Safi & Gumel, 2013)), the term "quarantine" was generally incorrectly used to refer to the removal of individuals who already have been infected with the disease (either in the exposed/latent (Day et al., 2006; Gumel et al., 2004; Safi & Gumel, 2010; Safi & Gumel, 2015), or even in the symptomatic (Hethcote et al., 2002; Nuño et al., 2005) class). In other words, the term "quarantine" was used instead of the more epidemiologically-appropriate term, "isolation". As stated earlier, quarantine is the temporary removal of susceptible individuals who are feared to have been exposed to a communicable

disease. These (currently-susceptible-but-feared-exposed) individuals are temporarily removed from the actively-mixing population until, at the very least, after the incubation period of the disease, after which they are tested to determine whether or not they have the disease. If they have acquired the infection, they are then placed in isolation. If they do not show clinical symptoms of the disease at the end of the quarantine period, they return to the susceptible (and actively-mixing) population. People can be quarantined at home (i.e., self-quarantine) or in public health facility (such as hospital, health centers or makeshift facility, such as the military tents used during the 2014 ebola outbreaks (Drazen et al., 2014)). Quarantine is correctly modeled in a few studies, including in (Lipsitch et al., 2003; Mubayi et al., 2010; Safi & Gumel, 2013). In particular, Lipsitch et al. (Lipsitch et al., 2003) modeled quarantine of susceptible individuals based on the number of individuals with clinical symptoms of the disease in the community. In addition to allowing for the quarantine of susceptible individuals, the model developed by Safi and Gumel (Safi & Gumel, 2013) also accounted for the adjustment of the disease incidence function to account for the actively-mixing population (in line with Hethcote (Hethcote et al., 2002)). These features were also incorporated in the model developed by Mubayi et al. (Mubayi et al., 2010). It is worth stating, however, that the quarantine models in (Lipsitch et al., 2003; Mubayi et al., 2010) do not allow breakthrough infection during quarantine. In other words, the models in (Lipsitch et al., 2003; Mubayi et al., 2010) assume perfect quarantine (this assumption is relaxed in the current study).

The purpose of the current study is to design a new model for realistically assessing the population-level impact of quarantine (assumed to be imperfect, so that individuals in quarantine can acquire infection during quarantine) on the spread and control of the 2014−2015 EVD outbreaks in the three affected Western African countries. The paper is organized as follows. The model is formulated and fitted with observed data in Section 2 (the basic properties of the model, as well as the local asymptotic stability result for the associated disease-free equilibrium, are also given). A special case of the model, in the absence of quarantine, is rigorously analysed in Section 3. Numerical simulations of the full model are reported in Section 5.

2. Formulation of mathematical model

The model is formulated as follows. The total population at time t, denoted by $N(t)$, is split into the population of those in quarantine (denoted by $N_Q(t)$) and those not in quarantine (denoted by $N_U(t)$), so that $N(t) = N_Q(t) + N_U(t)$. The total population of individuals in quarantine at time t is divided into those that are susceptible ($S_Q(t)$), exposed ($E_Q(t)$; that is, infected but not yet infectious) and symptomatic ($I_Q(t)$). Hence,

$$N_Q(t) = S_Q(t) + E_Q(t) + I_Q(t).$$

Similarly, the total population of individuals not in quarantine at time t is sub-divided into the sub-populations of susceptible ($S_U(t)$), exposed ($E_U(t)$), symptomatic ($I_U(t)$), treated ($I_T(t)$), recovered ($R(t)$), dead ($D(t)$), so that

$$N_U(t) = S_U(t) + E_U(t) + I_U(t) + I_T(t) + R(t) + D(t).$$

The *force of infection* associated with the model to be developed (denoted by $\lambda(t)$) is given by

$$\lambda(t) = \frac{I_U(t) + \eta_T I_T(t) + \eta_Q I_Q(t) + \eta_D D(t)}{N_U(t)}, \tag{1}$$

where η_T, η_Q and η_D are modification parameters accounting for the variability of the infectiousness of infected individuals in the I_T, I_Q and D classes, in comparison to those in the I_U class, respectively. Following Lipsitch et al. (Lipsitch et al., 2003), quarantine is modeled as follows: a fraction, q, of susceptible individuals who are feared exposed to Ebola (i.e., by having contact with a confirmed Ebola case) are placed in quarantine. Owing to its assumed imperfect nature, individuals in quarantine can be infected (and moved to the compartment E_Q) with probability b (quarantined individuals remain susceptible and stay in the quarantined susceptible S_Q class during quarantine with probability $1 - b$). Quarantined individuals who do not develop the disease at the end of the quarantine period are moved to the S_U class at a rate r_Q.
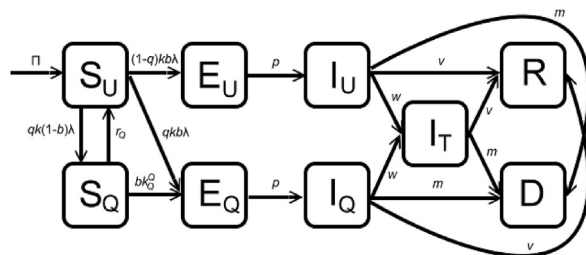

Fig. 1. Flow diagram of the model (2).

The model is given by the following deterministic system of nonlinear differential equations (where a prime denotes differentiation with respect to time t; a schematic diagram of the model is depicted in Fig. 1 and the parameters of the model are described in Table 1):

$$S'_U(t) = \Pi - kbS_U(t)\lambda(t) - qk(1-b)S_U(t)\lambda(t) + r_Q S_Q(t) - dS_U(t),$$

$$S'_Q(t) = qk(1-b)S_U(t)\lambda(t) - \frac{bk_Q^Q S_Q(t)I_Q(t)}{N_Q(t)} - r_Q S_Q(t) - dS_Q(t),$$

$$E'_U(t) = (1-q)kbS_U(t)\lambda(t) - pE_U(t) - dE_U(t),$$

$$E'_Q(t) = qkbS_U(t)\lambda(t) + \frac{bk_Q^Q S_Q(t)I_Q(t)}{N_Q(t)} - pE_Q(t) - dE_Q(t),$$ (2)

$$I'_U(t) = pE_U(t) - (v+m+w)I_U(t) - dI_U(t),$$

$$I'_T(t) = w\big(I_U(t) + I_Q(t)\big) - (v+m)I_T(t) - dI_T(t),$$

$$I'_Q(t) = pE_Q(t) - (v+m+w)I_Q(t) - dI_Q(t),$$

$$R'(t) = v\big(I_U(t) + I_T(t) + I_Q(t)\big) - dR(t),$$

$$D'(t) = m\big(I_U(t) + I_T(t) + I_Q(t)\big) - fD(t),$$

with the auxiliary equation

$$B'(t) = fD(t),$$

and $\lambda(t)$ as given by (1). In (2), Π is the recruitment rate (by birth or immigration), k is the average daily per capita contact rate in the community, b is the transmission probability *per* contact (here, we follow Lipsitch et al. (Lipsitch et al., 2003) in separating the parameters k and b instead of applying the usual composite transmission parameter β. That is, we assume that each infectious individual makes k contacts *per* day, and a proportion, b, of these contacts lead to infection). The parameters q and d represent, respectively, the quarantine rate of susceptible individuals and the natural mortality rate (the latter rate is assumed to be the same in all epidemiological compartments). Individuals in quarantine acquire EVD infection at a rate bk_Q^Q. The parameter p accounts for the rate of progression from any of the exposed classes (E_U or E_Q) to the corresponding symptomatic class (I_U or I_Q). That is, $1/p$ is the mean incubation period of the disease. Infectious individuals in the I_U and I_Q classes are hospitalized at a rate w. The parameters v and m are, respectively, the recovery rate and per capita disease-induced

Table 1
Description, ranges and baseline values of parameters of the model (2).

Parameter	Description	Baseline value (range)	Ref.
Π	Recruitment rate	11826/week	World Health Organization (2018c)
d	Natural death rate	0.00054/week	World Health Organization (2018c)
b	Transmission probability per contact	0.054	Legrand et al. (2007)
η_T	Modification parameter for infectiousness of hospitalized individuals	0.86	Legrand et al. (2007)
η_Q	Modification parameter for infectiousness of infected quarantined individuals	0.502 (0.5–0.9)	Legrand et al. (2007)
η_D	Modification parameter for infectiousness of Ebola-deceased individuals	3.89	Legrand et al. (2007)
k	Average per capita contact rate in the community	9.15/week	Legrand et al. (2007)
q	Quarantine rate of susceptible individuals	0.125 (0.05–0.5)/ week	Fitted
r_Q	Rate of release from quarantine	1.107 (0.5–2)/ week	Fitted
k_Q^Q	Average per capita contact rate during quarantine	7.97/week	Fitted
$1/p$	Incubation period	1.498 week	(Gomes et al., 2014; Legrand et al., 2007; Pandey et al., 2014)
v	Recovery rate	0.362/week	(Gomes et al., 2014; Legrand et al., 2007)
m	Ebola-induced death rate	0.797/week	(Gomes et al., 2014; Legrand et al., 2007; Pandey et al., 2014)
w	Hospitalization rate	1.58/week	(Gomes et al., 2014; Legrand et al., 2007; Rivers et al., 2014)
$1/f$	Mean time from death due to Ebola to burial	0.762 weeks	World Health Organization (2015)

death rate. Ebola-deceased individuals are buried at a rate f (i.e., $1/f$ is the mean time from death to burial for Ebola-deceased individuals) (Agusto et al., 2015; Barbarossa et al., 2015; Legrand et al., 2007). It is worth emphasizing that, in contrast to Lipsitch et al. (Lipsitch et al., 2003), it is assumed in this study that hospitalized individuals can transmit infection (hence, the mean duration of infectiousness is $1/(w + m + v)$).

The model (2) is an extension of many existing models for quarantine and isolation (such as those in (Gumel et al., 2004; Hethcote et al., 2002; Lipsitch et al., 2003; Mubayi et al., 2010; Nuño et al., 2005; Safi & Gumel, 2010; Safi & Gumel, 2013; Safi & Gumel, 2015; Yan & Zou, 2008)) by, *inter alia*:

1. Incorporating the quarantine of susceptible individuals (this was not included in the models in (Gumel et al., 2004; Hethcote et al., 2002; Nuño et al., 2005; Safi & Gumel, 2010; Safi & Gumel, 2015; Yan & Zou, 2008)).
2. Using nonlinear quarantine rate of susceptible individuals (linear rates were used in (Mubayi et al., 2010; Safi & Gumel, 2013)).
3. Allowing for breakthrough infection during quarantine (perfect quarantine and isolation were assumed in (Lipsitch et al., 2003; Mubayi et al., 2010). That is, the models in (Lipsitch et al., 2003; Mubayi et al., 2010) assume that susceptible individuals in quarantine do not acquire infection during the quarantine period).
4. Allowing for disease transmission by infected individuals in quarantine and/or isolation (this was not accounted for in the models in (Lipsitch et al., 2003; Mubayi et al., 2010)).
5. Allowing for the heterogeneity between infected individuals in quarantine and isolation and those not in quarantine and isolation (i.e., we stratify the infected population into E_Q and I_Q for those in quarantine and isolation, and E_U and I_U for those not in quarantine and isolation). This allows for the assessment of the effectiveness of an intervention strategy aimed at encouraging infected people in quarantine and isolation to positively modify their behavior so that they do not continue to generate more infections (this stratification is not considered in the model in (Mubayi et al., 2010). That is, all infected individuals are lumped into the same compartment in (Mubayi et al., 2010), regardless of their quarantine or isolation status).

Further, the model (2) extends many of the EVD models in the literature (such as those in (Agusto et al., 2015; Chowell et al., 2004; Tsanou et al., 2017)) by, *inter alia*, allowing for the quarantine of susceptible individuals and disease acquisition and transmission during quarantine and isolation (or hospitalization).

2.1. Basic qualitative properties

The basic qualitative properties of the model (2), with respect to the nonnegativity and boundedness of solutions, will now be explored.

Lemma 2.1. *Suppose that the initial values* $S_U(0), S_Q(0), E_U(0), E_Q(0), I_U(0), I_T(0), I_Q(0), R(0), D(0), B(0)$ *of the model (2) are all nonnegative. Then, the solution of (2) starting with these initial values will remain nonnegative for all time* $t > 0$. *Furthermore, all solutions of the model (2) are bounded.*

Proof. The proof for the nonnegativity component of the theorem is by contradiction (see Theorem A4 of (Thieme, 2003)). Suppose that the statement of the lemma (with respect to nonnegativity) does not hold. That is, there is at least one of the nine state variables of the model (2), and a $t = t^* \geq 0$, such that the value of this state variable goes through 0 at $t = t^*$, and all state variables of the model take nonnegative values for $0 \leq t \leq t^*$. For example, consider the state variable is $S_U(t)$. It can be seen that the derivative of $S_U(t)$ is positive if $S_U(t) = 0$. Hence, $S_U(t)$ cannot decrease further once it has reached 0. The case of each of the other state variable of the model can be shown in a similar way.

To show that all solutions of the model (2) are bounded, it is convenient to define $\mathscr{N}(t) = S_U(t) + S_Q(t) + E_U(t) + E_Q(t) + I_U(t) + I_T(t) + I_Q(t) + R(t) + D(t)$ and $\delta = \min\{f, d\}$. Thus,

$$\mathscr{N}'(t) = \Pi - d\big[S_U(t) + S_Q(t) + E_U(t) + E_Q(t) + I_U(t) + I_T(t) + I_Q(t) + R(t)\big] - fD(t)$$
$$\leq \Pi - \delta\mathscr{N}(t),$$

from which it follows that $\lim\sup_{t \to \infty} \mathscr{N}(t) \leq \frac{\Pi}{\delta}$. Using the fact that all solutions are nonnegative, the second statement of the lemma is established. ∎

Define the following feasible region for the model (2):

$$\Gamma = \left\{ (S_U(t), S_Q(t), E_U(t), E_Q(t), I_U(t), I_T(t), I_Q(t), R(t), D(t)) \in \mathbb{R}_+^9 : \mathscr{N}(t) \leq \frac{\Pi}{\delta} \right\}.$$

The result below follows from the above analyses.

Lemma 2.2. *The region* Γ *is positively-invariant for the model (2) for every nonnegative initial condition in* $\mathbb{R}_+^9$.

2.2. Data fitting

It should, first of all, be stated that good estimates for pretty much all the non-quarantine related parameters of the model (2) are available in the literature, as tabulated in Table 1. Further, good estimates for one of the four quarantine-related parameters (η_Q) are available. Thus, our task is to find good estimates for the remaining three quarantine-related parameters of the model (k_Q^Q, r_Q and q). In order to do so, and to subsequently validate the model, we fitted the model using the available cumulative data for the 2014–15 Ebola outbreaks in three affected West African countries. We apply Latin Hypercube Sampling (a Monte-Carlo sampling method used in statistics to measure simultaneous variation of several model parameters (McKay, Beckman, & Conover, 1979)) to generate a representative sample set from the parameter ranges for the three quarantine-related parameters (k_Q^Q, r_Q and q), while the baseline values for the rest of the parameters, given in Table 1, are used as well. For all elements of this representative sample set, we numerically calculate the solutions of the model (2) with the given parameter values and apply the least squares method to find the parameters which give the best fit. We consider the data of the first 40 weeks of the outbreak (World Health Organization, 2018d) (as tabulated in Table 2), as after this time, several intervention measures were implemented (hence, the estimates for many of the control-related parameters of the model, including the transmission, hospitalization and burial rates, changed significantly). The estimated values of the two quarantine-related parameters of the model obtained from the fitting exercise are tabulated in Table 1. The simulation results obtained for the cumulative number of cases, by fitting the model with the data of the first 40-week period, are depicted in Fig. 2. The figure shows a reasonably good fit (thereby adding realism to the predictive capacity of the model (2)). The goodness of the fit is theoretically measured by computing the associated *average relative error* of the fit using the formula $\frac{1}{40}\sum_{i=1}^{40}\frac{|y_i-\widehat{y_i}|}{|y_i|}\approx 0.8163$, where y_i and $\widehat{y_i}$ are the exact and estimated cumulative number of cases for Week i ($i = 1, 2, \cdots, 40$) (depicted in Table 2), respectively. The reasonably small value of the relative error (0.8134) confirms the goodness of the fit obtained.

Table 2
Cumulative number of cases reported (sum of confirmed, suspected and probable cases) in the first forty weeks of the 2014–2015 Ebola epidemic in Western Africa (World Health Organization, 2018d).

| Weeks	Guinea	Liberia	Sierra Leone
1	1	1	1
2	5	1	1
3	9	2	1
4	13	2	1
5	21	3	2
6	23	3	2
7	28	4	3
8	35	4	3
9	39	5	4
10	44	5	4
11	47	6	5
12	103	8	6
13	127	8	6
14	158	25	6
15	203	27	12
16	218	35	12
17	226	35	12
18	236	35	12
19	248	35	12
20	248	35	12
21	291	35	50
22	344	35	81
23	351	35	89
24	398	41	136
25	398	51	158
26	413	115	252
27	413	142	337
28	413	196	442
29	427	249	525
30	472	391	574
31	495	554	717
32	519	786	810
33	607	1082	910
34	648	1378	1026
35	771	1698	1216
36	899	2407	1478
37	942	3022	1673
38	1074	3458	2021
39	1199	3834	2437
40	1350	4076	2950
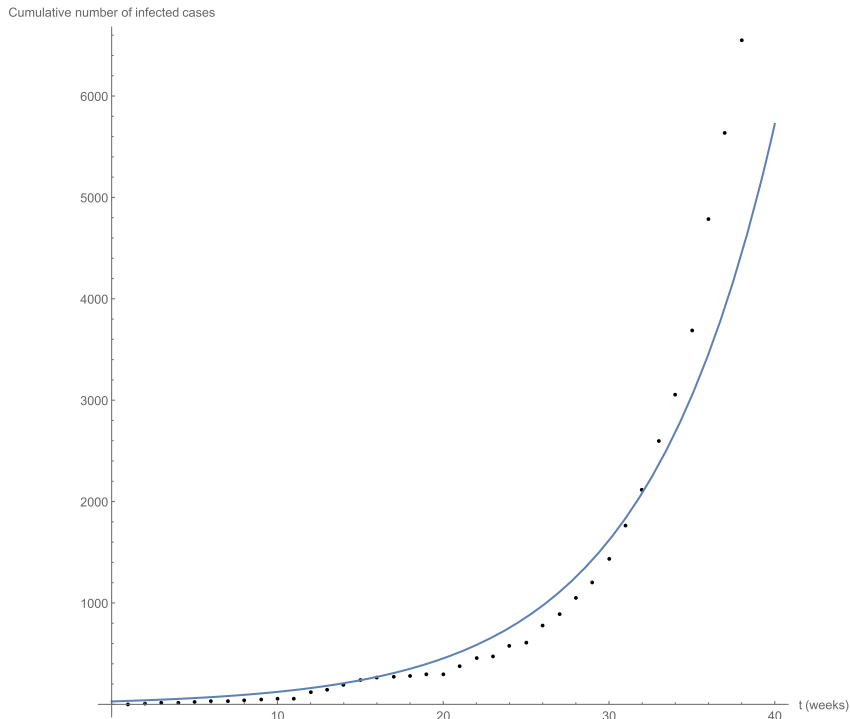
Fig. 2. Fitting the model to the data for the 2014–2015 Ebola outbreaks in Western Africa (World Health Organization, 2018d): cumulative number of new infected cases (Parameter values used are as given in Table 1).

3. Analysis of special case of the model: quarantine-free with mass action incidence

We consider, first of all, a special case of the model (2) in the absence of quarantine (i.e., the model (2) with $q = 0$) and constant total population (i.e., the model (2) with mass action incidence, rather than standard incidence). The two assumptions are made for mathematical tractability, in addition to allowing for the determination of whether or not adding quarantine to the resulting model (without quarantine) will alter its dynamical features. The second assumption of constant total population is justified since Ebola-induced mortality is generally very negligible, in comparison to the total population in the affected areas (World Health Organization, 2018d). The quarantine-free model with constant total population is given by:

$$
\begin{aligned}
S'_U(t) &= \Pi - kbS_U(t)I_U(t) - kb\eta_T S_U(t)I_T(t) - kb\eta_D S_U(t)D(t) - dS_U(t), \\
E'_U(t) &= kbS_U(t)I_U(t) + kb\eta_T S_U(t)I_T(t) + kb\eta_D S_U(t)D(t) - pE_U(t) - dE_U(t), \\
I'_U(t) &= pE_U(t) - (v + m + w)I_U(t) - dI_U(t), \\
I'_T(t) &= wI_U(t) - (v + m)I_T(t) - dI_T(t), \\
R'(t) &= v[I_U(t) + I_T(t)] - dR(t), \\
D'(t) &= m[I_U(t) + I_T(t)] - fD(t).
\end{aligned}
\tag{3}
$$

The reduced model (3) has a disease-free (trivial) equilibrium (DFE), $\mathscr{E}_0 = (S_U^*, E_U^*, I_U^*, I_T^*, R^*, D^*) = \left(\frac{\Pi}{d}, 0, 0, 0, 0, 0\right)$, and a non-trivial (positive) endemic equilibrium point (EEP)

$$
\mathscr{E}_1 = (S_U^{**}, E_U^{**}, I_U^{**}, I_T^{**}, R^{**}, D^{**})
$$

$$
= \left(\frac{\Pi - (d+p)E^*}{d}, E^*, \frac{pE^*}{d+m+v+w}, \frac{pwE^*}{(d+m+v)(d+m+v+w)}, \frac{pvE^*}{d(d+m+v)}, \frac{mpE^*}{f(d+m+v)}\right),
$$

where $E^* = \frac{1}{d+p}\left(1 - \frac{1}{\mathscr{R}_0}\right)$, with $\mathscr{R}_0$ (the basic reproduction number of the model (3)) given by

$$
\mathscr{R}_0 = \frac{\Pi bkp[d(f + \eta_D m) + f(m + v + \eta_T w) + \eta_D m(m + v + w)]}{df(d+p)(d+m+v)(d+m+v+w)}.
$$

The non-trivial equilibrium $\mathscr{E}_1$ exists whenever $\mathscr{R}_0 > 1$ (it should be noted that the S_U component of this equilibrium is positive for $\mathscr{R}_0 > 1$, since $1 - \frac{1}{\mathscr{R}_0} < 1$ and $\Pi > 1$).

3.1. Global asymptotic stability of equilibria

3.1.1. Disease-free equilibrium
The global asymptotic stability property of the DFE ($\mathscr{E}_0$) of the model (3) will be explored using the approach in [38, Theorem 2.1]. It is worth recalling the following result.

Theorem A.   ([(Shuai & van den Driessche, 2013), *Theorem 2.1*]).
  Consider the system

$$x' = \mathscr{F}(x, y) - \mathscr{V}(x, y),$$
$$y' = g(x, y) \tag{4}$$

with $g = (g_1, ..., g_m)^T$. The vectors $x = (x_1, ..., x_n) \in \mathbb{R}^n$ and $y = (y_1, ..., y_m)^T \in \mathbb{R}^m$ represent the populations in the disease compartments and the disease-free compartments, respectively. The functions $\mathscr{F}$ and $\mathscr{V}$ are defined as $\mathscr{F} = (\mathscr{F}_1, ..., \mathscr{F}_n)^T$ and $\mathscr{V} = (\mathscr{V}_1, ..., \mathscr{V}_n)^T$ such that $\mathscr{F}_i$ denotes the rate of new infections in the ith disease compartment and $\mathscr{V}_i$, $i = 1, ..., n$ denote transition terms. Assume that the disease-free system $y' = g(0, y)$ has a unique equilibrium $y_0 > 0$ which is locally asymptotically stable within the disease-free space. Define the two $n \times n$ matrices F and V as

$$F = \left(\frac{\partial \mathscr{F}_i}{\partial x_j}(0, y_0) \right) \quad \text{and} \quad V = \left(\frac{\partial \mathscr{V}_i}{\partial x_j}(0, y_0) \right),$$

and let,

$$\phi(x, y) := (F - V)x - \mathscr{F}(x, y) + \mathscr{V}(x, y).$$

Furthermore, let $\omega^T \geq 0$ be the left eigenvector of the matrix $V^{-1}F$ corresponding to the eigenvalue $\mathscr{R}_0$. If $\phi(x, y) \leq 0$ in $\Gamma \subset \mathbb{R}_+^{n+m}$, $F \geq 0$, $V^{-1} \geq 0$ and $\mathscr{R}_0 \leq 1$, then $Q = \omega^T V^{-1} x$ is a Lyapunov function for (4) on Γ.

Theorem 3.1.   *The disease-free equilibrium E_0 of the model (3) is globally-asymptotically stable in $\tilde{\Gamma} := \{(S_U(t), E_U(t), I_U(t), I_T(t), R(t), D(t)) \in \mathbb{R}_+^6\}$ whenever $\mathscr{R}_0 \leq 1$.*

Proof. Using the notation in Theorem A above, the next generation matrices, V and F, associated with the model (3) are given, respectively, by

$$V = \begin{pmatrix} d+p & 0 & 0 & 0 \\ -p & d+m+v+w & 0 & 0 \\ 0 & -w & d+m+v & 0 \\ 0 & -m & -m & f \end{pmatrix} \quad \text{and} \quad F = \begin{pmatrix} 0 & \dfrac{b\Pi k}{d} & \dfrac{b\Pi k\eta_T}{d} & \dfrac{bBk\eta_D}{d} \\ 0 & 0 & 0 & 0 \\ 0 & 0 & 0 & 0 \\ 0 & 0 & 0 & 0 \end{pmatrix},$$

and the function ϕ is given by

$$\phi(S_U, E_U, I_U, I_T, R, D)^T = \left(\frac{bk(\Pi - dS_U)(D\eta_D + \eta_T I_T + I_U)}{d}, 0, 0, 0 \right).$$

Hence, each condition of Theorem A is satisfied. Further, it follows from the above derivations that $\omega^T V^{-1} x$ is a Lyapunov function for (3), where ω is the left eigenvector of the matrix $V^{-1}F$ corresponding to the eigenvalue $\mathscr{R}_0$. The statement of the theorem follows from LaSalle's Invariance Principle (LaSalle & Lefschetz, 1961). ∎

3.1.2. Endemic equilibrium
The global asymptotic stability property of the endemic equilibrium $\mathscr{E}_1$ of the model (3) will be explored using results from (Shuai & van den Driessche, 2013). It is worth recalling the following result.

Theorem B.   ([(Shuai & van den Driessche, 2013), *Theorem 3.5*]).
  Let U be an open set in $\mathbb{R}^n$. Consider a differential equation system

$$z'_k = f_k(z_1, z_2, ..., z_m), \qquad k = 1, 2, ..., m, \tag{5}$$

with $z = (z_1, z_2, ..., z_m) \in U$.
Suppose the following assumptions are satisfied.

1. There exist functions $D_i : U \to \mathbb{R}$, $G_{ij} : U \to \mathbb{R}$ and constants $a_{ij} \geq 0$ such that for every $1 \leq i \leq n$, $D_i' = D_i'|_{(5)} \leq \sum_{j=1}^{n} a_{ij}G_{ij}(z)$ for $z \in U$.
2. For $A = [a_{ij}]$, each directed cycle $\mathscr{C}$ of the weighted digraph $\mathscr{G}$ defined by the weight matrix A has $\sum_{(s,r) \in \mathscr{E}(\mathscr{C})} G_{rs}(z) \leq 0$ for $z \in U$, where $\mathscr{E}(\mathscr{C})$ denotes the arc set of the directed cycle $\mathscr{C}$.

Then, there exist constants $c_i \geq 0$ such that the function $\mathscr{D}(z) = \sum_{i=1}^{n} c_i D_i(z)$ is a Lyapunov function for (5). We claim the following result.

Theorem 3.2. *The endemic equilibrium $\mathscr{E}_1$ of the model (3) is globally-asymptotically stable in*

$$\tilde{\mathbf{\Gamma}} \setminus \left\{ (S_U(t), E_U(t), I_U(t), I_T(t), R(t), D(t)) \in \mathbb{R}_+^6 : E_U(t) = I_U(t) = I_T(t) = D(t) = 0 \right\}$$

if $\mathscr{R}_0 > 1$.

Proof. Define $h : \mathbb{R} \to \mathbb{R}$ as $h(x) = x - 1 - \ln x$ and let $D_1 = h\left(\frac{S_U(t)}{S_U^{**}}\right) + \frac{E^{**}}{S_U^{**}} h\left(\frac{E_U(t)}{E^{**}}\right)$, $D_2 = h\left(\frac{I_U(t)}{I_U^{**}}\right)$, $D_3 = h\left(\frac{I_T(t)}{I_T^{**}}\right)$ and $D_4 = h\left(\frac{D(t)}{D^{**}}\right)$. At the endemic equilibrium, the following equalities hold:

$$\Pi = kbS_U^{**}I_U^{**} + kb\eta_T S_U^{**}I_T^{**} + kb\eta_D S_U^{**}D^{**} + dS_U^{**},$$

$$p + d = \frac{kbS_U^{**}I_U^{**} + kb\eta_T S_U^{**}I_T^{**} + kb\eta_D S_U^{**}D^{**}}{E^{**}},$$

$$v + m + w + d = p\frac{E^{**}}{I_U^{**}},$$

$$v + m + d = w\frac{I_U^{**}}{I_T^{**}},$$

$$f = m\frac{I_U^{**} + I_T^{**}}{D^{**}}.$$

Noting that $h(x) \geq 0$ for all $x > 0$ and $h(x) = 0$ if and only if $x = 1$, and applying the above equalities, gives:

$$D_1'(t) \leq kbI_U^{**}\left(\frac{I_U(t)}{I_U^{**}} - \ln\frac{I_U(t)}{I_U^{**}} - \frac{E_U(t)}{E^{**}} - \ln\frac{E_U(t)}{E^{**}}\right)$$

$$+ kb\eta_T I_T^{**}\left(\frac{I_T(t)}{I_T^{**}} - \ln\frac{I_T(t)}{I_T^{**}} - \frac{E_U(t)}{E^{**}} - \ln\frac{E_U(t)}{E^{**}}\right)$$

$$+ kb\eta_D D^{**}\left(\frac{D(t)}{D^{**}} - \ln\frac{I_U(t)}{I_U^{**}} - \frac{E_U(t)}{E^{**}} - \ln\frac{E_U(t)}{E^{**}}\right)$$

$$:= a_{12}G_{12} + a_{13}G_{13} + a_{14}G_{14},$$

$$D_2'(t) \leq p\frac{E^{**}}{I_U^{**}}\left(\frac{E_U(t)}{E^{**}} - \ln\frac{E_U(t)}{E^{**}} - \frac{I_U(t)}{I_U^{**}} - \ln\frac{I_U(t)}{I_U^{**}}\right) := a_{21}G_{21},$$

$$D_3'(t) \leq w\frac{I_U^{*}}{I_T^{**}}\left(\frac{I_U(t)}{I_U^{**}} - \ln\frac{I_U(t)}{I_U^{**}} - \frac{I_T(t)}{I_T^{**}} - \ln\frac{I_T(t)}{I_T^{**}}\right) := a_{32}G_{32},$$

and,

$$D_4'(t) \leq \frac{mI_U^{**}}{D^{**}}\left(\frac{I_U(t)}{I_U^{**}} - \ln\frac{I_U(t)}{I_U^{**}} - \frac{D(t)}{D^{**}} - \ln\frac{D(t)}{D^{**}}\right)$$

$$+ \frac{mI_T^{**}}{D^{**}}\left(\frac{I_T(t)}{I_T^{**}} - \ln\frac{I_T(t)}{I_T^{**}} - \frac{D(t)}{D^{**}} - \ln\frac{D(t)}{D^{**}}\right),$$

$$:= a_{43}G_{43} + a_{42}G_{42}.$$

Hence, Assumption (1) of Theorem B holds. Define the weighted digraph $(\mathscr{G}, A)$ associated with the weight matrix $A = [a_{ij}]$, with a_{ij} defined as the constants in the above inequalities (and all other a_{ij}'s not mentioned above are set to zero; see also Fig. 3).

For all cycles of $(\mathscr{G}, A)$, the Assumption (2) of Theorem B can easily be verified. For instance, the case of the cycle ① → ② → ③ → ④ is verified as follows. For this cycle,

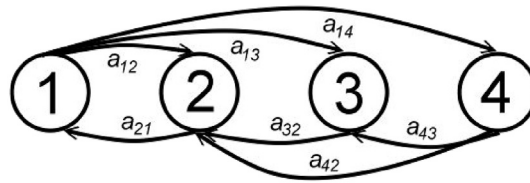**Fig. 3.** The weighted digraph $(\mathscr{G}, A)$ constructed for model (3).

$$G_{14} + G_{43} + G_{32} + G_{21}$$

$$= \left(\frac{D(t)}{D^{**}} - \ln \frac{I_U(t)}{I_U^{**}} - \frac{E_U(t)}{E^{**}} - \ln \frac{E_U(t)}{E^{**}} \right) + \left(\frac{I_T(t)}{I_T^{**}} - \ln \frac{I_T(t)}{I_T^{**}} - \frac{D(t)}{D^{**}} - \ln \frac{D(t)}{D^{**}} \right)$$

$$+ \left(\frac{I_U(t)}{I_U^{**}} - \ln \frac{I_U(t)}{I_U^{**}} - \frac{I_T(t)}{I_T^{**}} - \ln \frac{I_T(t)}{I_T^{**}} \right) + \left(\frac{E_U(t)}{E^{**}} - \ln \frac{E_U(t)}{E^{**}} - \frac{I_U(t)}{I_U^{**}} - \ln \frac{I_U(t)}{I_U^{**}} \right)$$

$$= 0.$$

The other cases can be handled in a similar way. Hence, the statement of the theorem follows from Theorem B.

It is worth stating that, using the baseline values of the parameters in Table 1, the value of the basic reproduction number $(\mathscr{R}_0)$ is $\mathscr{R}_0 = 1.403 > 1$ (hence, it follows from Theorem 3.2 that the disease will persist in the population). It is further worth noting that this value of $\mathscr{R}_0$ lies in the range given in numerous modeling studies for the 2014 EVD outbreaks (such as those in (Agusto et al., 2015; Barbarossa et al., 2015; Gomes et al., 2014; Nishiura & Chowell, 2014; Towers et al., 2014)).

4. Analysis of full model with quarantine and standard incidence

In this section, the local asymptotic stability of the DFE of the full model (2) (with both quarantine and standard incidence) will be analysed. The DFE of the full model is given by:

$$\mathscr{E}_{01} = \left(S_U^*, S_Q^*, E_U^*, E_Q^*, I_U^*, I_T^*, I_Q^*, R^*, D^* \right) = \left(\frac{\Pi}{d}, 0, 0, 0, 0, 0, 0, 0, 0 \right),$$

and it can be shown (using the next generation operator method (Diekmann, Heesterbeek, & Roberts, 2010; van den Driessche & Watmough, 2002)) that the associated *quarantine reproduction number*, denoted by $\mathscr{R}_0^Q$, is given by:

$$\mathscr{R}_0^Q = \frac{bkp\big[m\eta_D(m + v + w + d) + qf(m\eta_Q + v\eta_Q + d\eta_Q + w\eta_T) + (1-q)f(m + v + w\eta_T + d)\big]}{f(d+p)(d+m+v)(d+m+v+w)}.$$

The result below follows from Theorem 2 of (van den Driessche & Watmough, 2002).

Theorem 4.1. *The DFE of the full model* (2), $\mathscr{E}_{01}$, *is locally-asymptotically stable if* $\mathscr{R}_0^Q < 1$, *and is unstable if* $\mathscr{R}_0^Q > 1$.

As in (Safi and Gumel, 2013, 2015), the model (2) can be shown (using standard tools, such as the centre manifold theory (Castillo-Chavez & Song, 2004)) to undergo the phenomenon of backward bifurcation at $\mathscr{R}_0^Q = 1$, a dynamic phenomenon associated with the co-existence of stable disease-free equilibrium and a stable endemic equilibrium when the associated reproduction threshold, $\mathscr{R}_0^Q$, is less than unity. The epidemiological implication of this phenomenon, which arises due to the imperfect nature of quarantine to prevent disease transmission during quarantine (i.e., leaky quarantine), is that having $\mathscr{R}_0^Q < 1$, while necessary, is no longer sufficient for the effective control of the disease. In other words, quarantine-induced backward bifurcation makes the effort for the effective control of Ebola more difficult. Hence, this study shows that adding imperfect quarantine to the quarantine-free Ebola transmission model (3) induces a new dynamical phenomenon (backward bifurcation) that was not present in the quarantine-free model.

4.1. Uncertainty and sensitivity analysis

The model (2) contains numerous parameters, and uncertainties are expected to arise in the estimates of the parameter values used in the model simulations. Uncertainty analysis, using Latin Hypercube Sampling (LHS) (Blower & Dowlatabadi, 1994), is used to account for such uncertainty. The baseline values and ranges of the parameters in Table 1 are used for this analysis, and it is assumed each parameter of the model obeys a uniform distribution. Using the quarantine reproduction number $(\mathscr{R}_0^Q)$ as the response function, the results for the uncertainty analysis obtained show that $\mathscr{R}_0^Q$ lies in the range (0.268,

(a) Parameter values used are as given in Table 1

(b) Parameter values used are as given in Table 1 with $\eta_Q = 0$

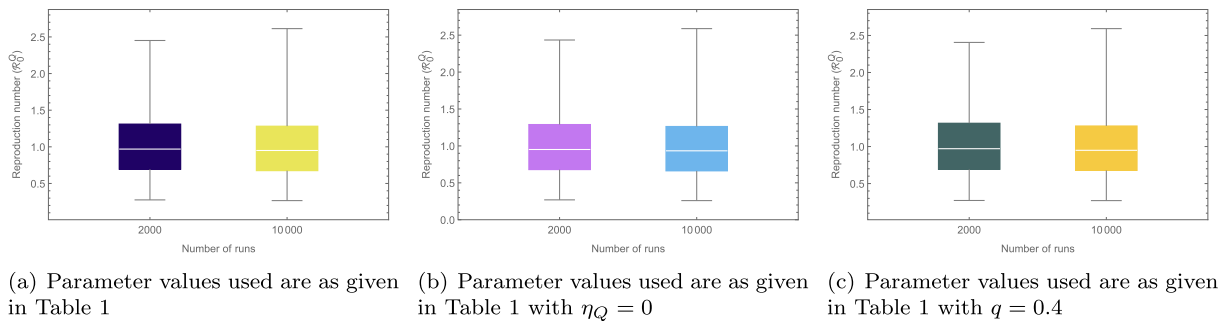(c) Parameter values used are as given in Table 1 with $q = 0.4$

Fig. 4. Box plot of the reproduction number ($\mathscr{R}_0^Q$) with 2000, resp. 10000 LHS runs. Parameter values used are as given in Table 1.

2.585), with a mean $1.013 > 1$ (Fig. 4(a)). This simulation suggests that, although the community-wide implementation of quarantine significantly reduces the basic reproduction number ($\mathscr{R}_0 = 1.403$ in this case), this level (and effectiveness) of quarantine is unable to lead to the effective control of the disease (since $\mathscr{R}_0^Q > 1$, *albeit* only slightly). However, if the parameter η_Q, for the reduction of infectiousness of quarantined-infected individuals, is further reduced from its baseline value (e.g., if it is reduced from 0.502 to 0), the mean value of $\mathscr{R}_0^Q$ reduces to $0.997 < 1$ (so that effective disease control is feasible in this case) (see Fig. 4(b)). Similarly, increasing the quarantine rate (q) from the current baseline value of $q = 0.125$ to $q = 0.4$, for instance, leads to a reduction of mean $\mathscr{R}_0^Q$ from $\mathscr{R}_0^Q = 1.009$ to $\mathscr{R}_0^Q = 0.997$ (see Fig. 4(c)). In other words, these simulations show that the singular implementation of quarantine strategy in the community can lead to the effective control (or elimination) of the disease if the coverage (q) and effectiveness of quarantine to prevent transmission during quarantine (i.e., reduce η_Q) is high enough.

Furthermore, sensitivity analysis is carried out, using Partial Rank Correlation Coefficients (PRCCs (Blower & Dowlatabadi, 1994)), to determine the parameters of the model (2) that have the highest impact on the disease dynamics. For these simulations, the cumulative number of new cases is chosen as the response function. The sensitivity analysis based on the PRCC ranks the effect of the parameters on the response function (or outcome), while varying the parameters in their given ranges (parameters with higher positive (negative) PRCC values are positively (negatively) correlated with the response function). Table 3 depicts the resulting PRCC values obtained for the parameters of the model, from which it follows that the average contact rate in the community (k) and the probability of transmission per contact (b) are the most dominant parameters that affect the response function (the cumulative number of cases). The mean length of time for the burial of Ebola-deceased individuals ($1/f$) is also shown to be influential, as expected (having the third highest PRCC value in magnitude). Further, of the quarantine-related parameters, those related to the quarantine of susceptible individuals (q) and the reduction of the infectiousness of quarantined-infected individuals (η_Q^Q) are also influential (*albeit* with significantly decreased PRCC values in magnitude in comparison to the PRCC values of k and b). Thus, this study suggests that a quarantine program that significantly decreases the value of η_Q^Q (which can be achieved by effectively treating infected quarantined individuals and/or limiting their contacts with susceptible individuals during quarantine) or increase q (by increasing the contact tracing and quarantining of people feared exposed to EVD infection) can lead to a significant reduction in disease burden.

Table 3
Partial rank correlation coefficients of parameters of model 2.

Parameter	Description	PRCC
b	Transmission probability *per* contact	0.72
k	Average per capita contact rate in the community	0.78
q	Quarantine rate of susceptible individuals	−0.23
η_T	Modification parameter for infectiousness of hospitalized individuals	−0.18
η_Q	Modification parameter for infectiousness of infected quarantined individuals	−0.19
η_D	Modification parameter for infectiousness of Ebola-deceased individuals	0.35
$1/r_Q$	Length of stay in quarantine	0.23
k_Q^Q	Average per capita contact rate during quarantine	−0.19
$1/p$	Incubation period	0.22
v	Recovery rate	−0.08
m	Ebola-induced death rate	−0.39
w	Hospitalization rate	−0.24
$1/f$	Mean time from death due to Ebola to burial	0.43

5. Numerical simulations

Further numerical simulations are carried out to assess the population-level impact of the quarantine-related parameters of the model (2). These simulations show, in particular, that while the quarantine of susceptible individuals (q) and the average duration in quarantine ($1/r_Q$) have marginal impact on the cumulative number of new Ebola cases (Figs. 5 and 6, respectively), the modification parameter for transmission during quarantine (η_Q) and the contact rate during quarantine (k_Q^Q) have significant impact on the disease burden (Figs. 7 and 8, respectively). In other words, these simulations show that the parameters related to the efficacy of quarantine (η_Q and k_Q^Q) play a more significant role on the disease dynamics than the parameters related to quarantine rate of susceptible individuals (q) and length of quarantine (r_Q). A contour plot of the quarantine reproduction number ($\mathscr{R}_0^Q$), as a function of η_Q and q, is depicted in Fig. 9, from which it follows that $\mathscr{R}_0^Q$ decreases with decreasing values of η_Q and increasing values of q. Hence, this plot further supports the earlier result that the implementation of a quarantine strategy that reduces the infectiousness of quarantined-infected individuals (coupled with increased quarantine rate, q) will result in significant reduction of disease burden in the community.

6. Discussion and conclusion

Quarantine of individuals suspected of being exposed to a contagious disease is one of the oldest public health measures for combatting the spread of such contagious diseases in populations. This study presents a new deterministic model for
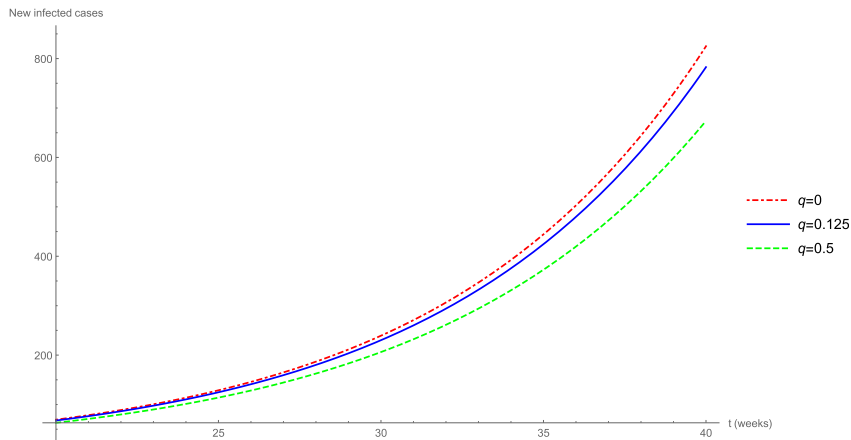

Fig. 5. Effect of quarantine of susceptible individuals (q) on the number of new Ebola cases. Parameter values used are as given in Table 1, with different values of q.
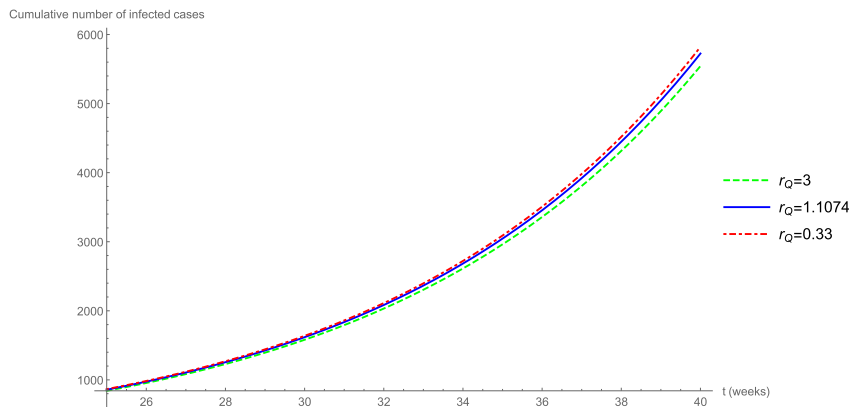

Fig. 6. Effect of duration of quarantine ($1/r_Q$) on the cumulative number of new Ebola cases. Parameter values used are as given in Table 1, with $r_Q = 0.33$, $r_Q = 1.54$ (fitted value) and $r_Q = 3$.
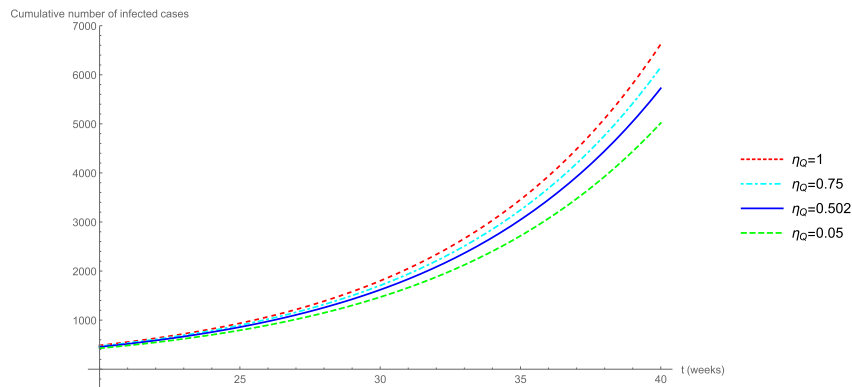
Fig. 7. Effect of modification parameter for disease transmission during quarantine (η_Q) on the cumulative number of new Ebola cases. Parameter values used are as given in Table 2, with $\eta_Q = 0.05, \eta_Q = 0.502$ (fitted value), $\eta_Q = 0.75$ and $\eta_Q = 1$.
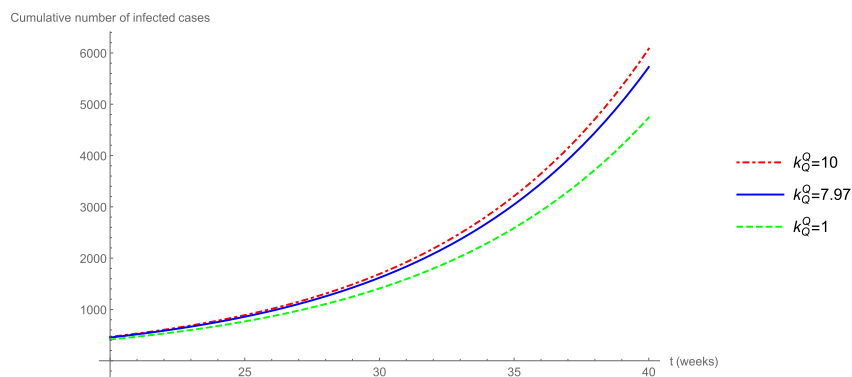

Fig. 8. The effect of the per capita contact rate (k_Q^Q) during quarantine.

assessing the population-level impact of the implementation of quarantine on the control of the 2014 Ebola outbreaks in West Africa. The model was fitted using data relevant to the EVD dynamics in Guinea, Liberia and Sierra Leone. Some of the notable features of the model include the explicit modeling of quarantine of both susceptible and infected individuals (in line with the approach by Lipsitch et al. (Lipsitch et al., 2003)) and the assumption that quarantine is imperfect (so that disease transmission can occur during quarantine). Detailed theoretical analysis of a special case of the model, in the absence of quarantine and with constant total population, was carried out. The analysis revealed that the disease-free equilibrium of the resulting quarantine-free model is globally-asymptotically stable whenever a certain epidemiological quantity (the basic reproduction number of the model, denoted by $\mathscr{R}_0$) is less than unity. The epidemiological implication of this result is that, in the absence of quarantine, bringing $\mathscr{R}_0$ to a value less than unity is necessary and sufficient for the effective control of the disease in the population. The quarantine-free model is also shown to have a unique endemic equilibrium (where Ebola persists in the population), which is globally-asymptotically stable, whenever $\mathscr{R}_0 > 1$. The full model with quarantine was also analysed, from which it was deduced that adding imperfect quarantine to the quarantine-free model introduces a dynamic phenomenon (backward bifurcation) that was not present in the former model. Thus, the community-wide implementation of imperfect quarantine measures (except if implemented with high efficacy to minimize disease transmission during quarantine) may fail to lead to the effective control of the disease. The presence of backward bifurcation in the transmission dynamics of a disease makes its effective control more difficult (since a lot more effort is needed to reduce the associated reproduction number further below unity, outside the backward bifurcation region).

Detailed uncertainty and sensitivity analysis are carried out on the parameters of the model to assess the impact of uncertainties in the estimates of parameter values (on the numerical simulation results obtained) and determine the parameters that are most influential to the disease transmission dynamics (as measured in terms of the cumulative number of new infections). It was shown that while the current level and efficacy of quarantine significantly reduces the value of the basic reproduction number ($\mathscr{R}_0$) of the model (hence, significantly reduces disease burden), it fails to bring this number to a value less than one (so that disease elimination is feasible). However, a modest increase in quarantine rate and/or the effectiveness level of quarantine (with respect to either reduction in the infectiousness of quarantined-infected individuals (η_Q) or
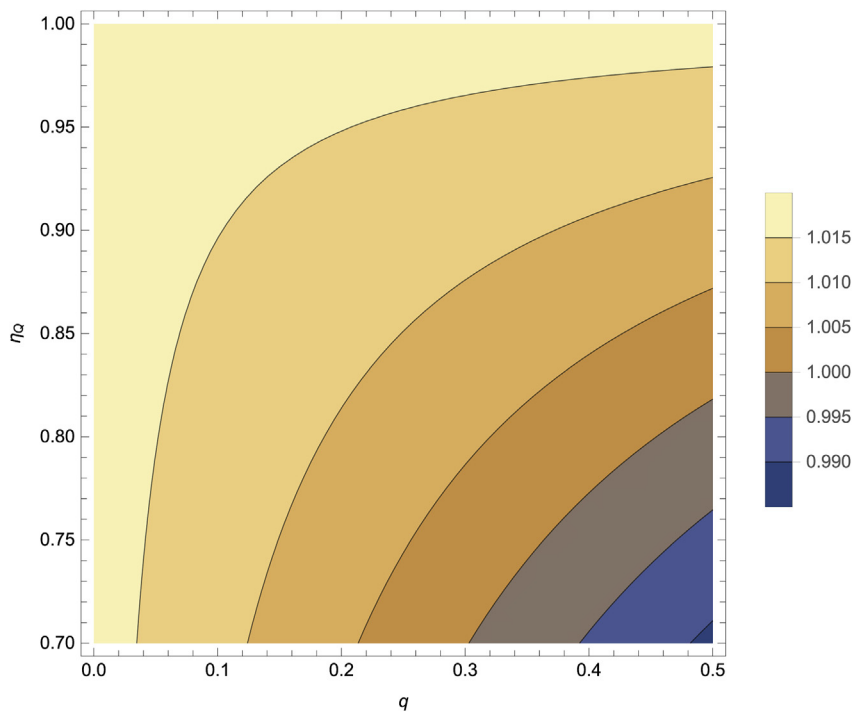
Fig. 9. Contour plot of the quarantine reproduction number ($\mathscr{R}_0^Q$), as a function of modification parameter for reduction of infectiousness of quarantined-infected individuals (η_Q) and contact rate during quarantine (k_Q^Q). Parameter values used are as given in Table 1, with $b = 0.054$, $k = 9.3$, $\eta_T = 0.7176$, $\eta_D = 2.748$, $p = 0.6784$, $v = 0.4764$, $m = 0.8578$, $w = 1.3578$, $f = 1.276$ and $d = 0.00054$.

minimizing contact during quarantine (k_Q^Q)) can reduce the quarantine reproduction number of the model ($\mathscr{R}_0^Q$) to a value less than one (thereby making effective disease control or elimination feasible).

The results of the sensitivity analysis carried out show that the contact rate in the community (k), transmission probability per contact (b) and the mean duration before burying Ebola-deceased individuals ($1/f$) have the most influence on the disease burden (as measured in terms of the cumulative number of new cases). Thus, these simulation results suggest that control measures that decrease the impact of these parameters (e.g., minimizing contacts with people suspected of the disease or reducing the time before an Ebola-deceased individual is buried) will be quite effective in minimizing disease burden. Our results suggest that the quarantine of susceptible individuals and the average duration in quarantine have a smaller effect on the number of infected, the modified transmission rate during quarantine and the contact rate for quarantined people have an important effect on the spread of the disease. The results of this study show that the prospects of the effective control of EVD using quarantine alone are bright, provided the coverage and effectiveness levels are high enough.

Declaration of conflict of interest

The authors declare no conflict of interest.

Acknowledgements

Appendix A. Supplementary data

Supplementary data to this article can be found online at https://doi.org/10.1016/j.idm.2019.01.003.

References

Agusto, F. B., Teboh-Ewungkem, M. I., & Gumel, A. B. (2015). Mathematical assessment of the effect of traditional beliefs and customs on the transmission dynamics of the 2014 Ebola outbreaks. *BMC Medicine, 13*(1), 96. https://doi.org/10.1186/s12916-015-0318-3.

Althaus, C. L. (2014). Estimating the reproduction number of Ebola virus (EBOV) during the 2014 outbreak in West Africa. *PLoS Currents Outbreaks, 6*. https://doi.org/10.1371/currents.outbreaks.91afb5e0f279e7f29e7056095255b288. . (Accessed 2 September 2014), 1.

Barbarossa, M. V., Dénes, A., Kiss, G., Nakata, Y., Röst, G., & Vizi, Z. (2015). Transmission dynamics and final epidemic size of Ebola Virus Disease outbreaks with varying interventions. *PLoS One, 10*(7), e0131398. https://doi.org/10.1371/journal.pone.0131398.

Blower, S. M., & Dowlatabadi, H. (1994). Sensitivity and uncertainty analysis of complex models of disease transmission: An HIV model, as an example. *International Statistical Review, 62*, 229—243. https://doi.org/10.2307/1403510.

Bowen, E. T. W., Platt, G. S., Lloyd, G., Baskerville, A., Harris, W. J., & Vella, E. E. (1977). Viral haemorrhagic fever in southern Sudan and northern Zaire. Preliminary studies on the aetiological agent. *Lancet, 309*, 571—573. https://doi.org/10.1016/S0140-6736(77)92001-3.

Campbell, L., Adan, C., & Morgado, M. (2017). *Learning from the Ebola response in cities: Responding in the context of quarantine*. ALNAP Working Paper. London: ALNAP/ODI.

Castillo-Chavez, C., & Song, B. (2004). Dynamical models of tuberculosis and their applications. *Mathematical Biosciences and Engineering, 1*(2), 361—404. https://doi.org/10.3934/mbe.2004.1.361.

Chowell, G., Hengartner, N. W., Castillo-Chavez, C., Fenimore, P. W., & Hyman, J. M. (2004). The basic reproductive number of Ebola and the effects of public health measures: The cases of Congo and Uganda. *Journal of Theoretical Biology, 229*(1), 119—126. https://doi.org/10.1016/j.jtbi.2004.03.006.

Day, T., Park, A., Madras, N., Gumel, A., & Wu, J. (2006). When is quarantine a useful control strategy for emerging infectious diseases? *American Journal of Epidemiology, 163*(5), 479—485. https://doi.org/10.1093/aje/kwj056.

Diekmann, O., Heesterbeek, J. A. P., & Roberts, M. G. (2010). The construction of next-generation matrices for compartmental epidemic models. *Journal of The Royal Society Interface, 7*(47), 873—885. https://doi.org/10.1098/rsif.2009.0386.

Drazen, J. M., Kanapathipillai, R., Campion, E. W., Rubin, E. J., Hammer, S. M., Morrissey, S., et al. (2014). Ebola and quarantine. *New England Journal of Medicine, 371*, 2029—2030. https://doi.org/10.1056/NEJMe1413139.

van den Driessche, P., & Watmough, J. (2002). Reproduction numbers and sub-threshold endemic equilibria for compartmental models of disease transmission. *Mathematical Biosciences, 180*, 29—48. https://doi.org/10.1016/S0025-5564(02)00108-6.

Eba, P. M. (2014). Ebola and human rights in West Africa. *The Lancet, 384*(9960), 2091—2093. https://doi.org/10.1016/S0140-6736(14)61412-4.

Gomes, M. F., Pastore y Piontti, A., Rossi, L., Chao, D., Longini, I., Halloran, M. E., et al. (2014). Assessing the international spreading risk associated with the 2014 West African Ebola outbreak. *PLoS Currents Outbreaks, 6*. https://doi.org/10.1371/currents.outbreaks.cd818f63d40e24aef769dda7df9e0da5. . (Accessed 2 September 2014). Edition 1.

Gumel, A., Ruan, S., Day, T., Watmough, J., Brauer, F., van den Driesche, P., et al. (2004). Modelling strategies for controlling SARS outbreaks. *Proceedings of the Royal Society of London B Biological Sciences, 271*. https://doi.org/10.1098/rspb.2004.2800, 2233—2232.

Haas, C. N. (2014). On the quarantine period for Ebola virus. *PLoS Currents Outbreaks, 6*. https://doi.org/10.1371/currents.outbreaks.2ab4b76ba7263ff0-f084766e43abbd89. . (Accessed 14 October 2014). Edition 1.

Hethcote, H., Zhien, M., & Shengbing, L. (2002). Effects of quarantine in six endemic models for infectious diseases. *Mathematical Biosciences, 180*, 141—160. https://doi.org/10.1016/S0025-5564(02)00111-6.

Johnson, K. M., Webb, P. A., Lange, J. V., & Murphy, F. A. (1977). Isolation and partial characterisation of a new virus causing acute haemorrhagic fever in Zaire. *Lancet, 309*, 569—571. https://doi.org/10.1016/S0140-6736(77)92000-1.

LaSalle, J., & Lefschetz, S. (1961). Stability by Liapunov's direct method, with applications. In *Mathematics in science and engineering* (Vol. 4)New York-London: Academic Press.

Legrand, J., Grais, R. F., Boelle, P.-Y., Valleron, A.-J., & Flahault, A. (2007). Understanding the dynamics of Ebola epidemics. *Epidemiology and Infection, 135*(4), 610—621. https://doi.org/10.1017/S0950268806007217.

Lewnard, J. A., Mbah, M. L. N., Alfaro-Murillo, J. A., Altice, F. L., Bawo, L., Nyenswah, T. G., et al. (2014). Dynamics and control of Ebola virus transmission in Montserrado, Liberia: A mathematical modelling analysis. *The Lancet Infectious Diseases, 14*(12), 1189—1195. https://doi.org/10.1016/S1473-3099(14)70995-8.

Lipsitch, M., Cohen, T., Cooper, B., Robins, J. M., Ma, S., James, L., et al. (2003). Transmission dynamics and control of severe acute respiratory syndrome. *Science, 300*(5627), 1966—1970. https://doi.org/10.1126/science.1086616.

McKay, M. D., Beckman, R. J., & Conover, W. J. (1979). A comparison of three methods for selecting values of input variables in the analysis of output from a computer code. *Technometrics, 21*(2), 239—245. https://doi.org/10.2307/1268522.

Mubayi, A., Kribs Zaleta, C., Martcheva, M., & Castillo-Chávez, C. (2010). A cost-based comparison of quarantine strategies for new emerging diseases. *Mathematical Biosciences and Engineering, 7*(3), 687—717. https://doi.org/10.3934/mbe.2010.7.687.

Nishiura, H., & Chowell, G. (2014). Early transmission dynamics of Ebola virus disease (EVD), West Africa, March to August 2014. *Euro Surveillance, 19*(36), 20894. https://doi.org/10.2807/1560-7917.ES2014.19.36.20894.

Nuño, M., Feng, Z., Martcheva, M., & Castillo-Chavez, C. (2005). Dynamics of two-strain influenza with isolation and partial cross-immunity. *SIAM Journal on Applied Mathematics, 65*(3), 964—982. https://doi.org/10.1137/S003613990343882X.

Pandey, A., Atkins, K. E., Medlock, J., Wenzel, N., Townsend, J. P., Childs, J. E., et al. (2014). Strategies for containing Ebola in West Africa. *Science, 346*(6212), 991—995. https://doi.org/10.1126/science.1260612.

Rivers, C. M., Lofgren, E. T., Marathe, M., Eubank, S., & Lewis, B. L. (2014). Modeling the impact of interventions on an epidemic of Ebola in Sierra Leone and Liberia. *PLoS Currents Outbreaks, 6*. https://doi.org/10.1371/currents.outbreaks.4d41fe5d6c05e9df30ddce33c66d084c. . (Accessed 6 November 2014). Edition 2.

Safi, M. A., & Gumel, A. B. (2010). Global asymptotic dynamics of a model for quarantine and isolation. *Discrete and Continuous Dynamical Systems - Series B, 14*(1), 209—231. https://doi.org/10.3934/dcdsb.2010.14.209.

Safi, M. A., & Gumel, A. B. (2013). Dynamics of a model with quarantine-adjusted incidence and quarantine of susceptible individuals. *Journal of Mathematical Analysis and Applications, 399*(2), 565—575. https://doi.org/10.1016/j.jmaa.2012.10.015.

Safi, M. A., & Gumel, A. B. (2015). Dynamics analysis of a quarantine model in two patches. *Mathematical Methods in the Applied Sciences, 38*(2), 349—364. https://doi.org/10.1002/mma.3072.

Shuai, Z., & van den Driessche, P. (2013). Global stability of infectious disease models using Lyapunov functions. *SIAM Journal on Applied Mathematics, 73*(4), 1513—1532. https://doi.org/10.1137/120876642.

Thieme, H. R. (2003). *Mathematics in population biology, Princeton Series in Theoretical and Computational Biology*. Princeton, NJ: Princeton University Press.

Towers, S., Patterson-Lomba, O., & Castillo-Chavez, C. (2014). Temporal variations in the effective reproduction number of the 2014 West Africa Ebola outbreak. *PLoS Currents Outbreaks, 6*. https://doi.org/10.1371/currents.outbreaks.9e4c4294ec8ce1adad283172b16bc908. . (Accessed 18 September 2014). Edition 1.

Tsanou, B., Bowong, S., Lubuma, J., & Mbang, J. (2017). Assessing the impact of the environmental contamination on the transmission of Ebola virus disease (EVD). *Journal of Applied Mathematics and Computing, 55*(1—2), 205—243. https://doi.org/10.1007/s12190-016-1033-8.

Tsanou, B., Lubuma, J., Ouemba Tassé, A. J., & Tenkam, H. M. (2018). Dynamics of host-reservoir transmission of Ebola with spillover potential to humans. *Electronic Journal of Qualitative Theory of Differential Equations*. https://doi.org/10.14232/ejqtde.2018.1.14. Paper No. 14, 32.

Webb, G. F., & Browne, C. J. (2016). A model of the Ebola epidemics in West Africa incorporating age of infection. *Journal of Biological Dynamics, 10*(1), 18—30. https://doi.org/10.1080/17513758.2015.1090632.

World Health Organization. (2015). *WHO One year into the ebola epidemic: A deadly, tenacious and unforgiving virus*. . (Accessed 8 April 2018). http://www.who.int/csr/disease/ebola/one-year-report/introduction/en.

World Health Organization. (2018a). *WHO Ebola virus disease*. . (Accessed 8 April 2018). http://www.who.int/mediacentre/factsheets/fs103/en/.

World Health Organization. (2018b). *WHO Ebola situation reports: Democratic Republic of the Congo*. . (Accessed 22 October 2018). http://www.who.int/ebola/situation-reports/drc-2018/en/.

World Health Organization. (2018c). *WHO Global Health Observatory data repository. Crude birth and death rate. Data by country*. . (Accessed 8 April 2018). http://apps.who.int/gho/data/node.main.CBDR107?lang=en.

World Health Organization. (2018d). *WHO Ebola data and statistics*. . (Accessed 13 April 2018). http://apps.who.int/gho/data/node.ebola-sitrep.

Yan, X., & Zou, Y. (2008). Optimal and sub-optimal quarantine and isolation control in SARS epidemics. *Mathematical and Computer Modelling, 47*(1–2), 235–245. https://doi.org/10.1016/j.mcm.2007.04.003.